Original Article

The molecular mechanism of sepsis-induced diaphragm dysfunction

Xiaosa Yuan[1#], Fangsu Xue[2#], Yunchi Yu[1], Xiaowen Cao[1], Yimin Han[3], Fei Wang[1], Lou Zhong[1]

[1]Department of Thoracic Surgery, Affiliated Hospital of Nantong University, Nantong, China; [2]Department of Respiration, Binhai County People's Hospital, Yancheng, China; [3]Department of Pediatrics, Medical College, Nantong University, Nantong, China

Contributions: (I) Conception and design: L Zhong; (II) Administrative support: L Zhong; (III) Provision of study materials or patients: X Yuan, F Xue, Y Yu, X Cao, Y Han, F Wang; (IV) Collection and assembly of data: X Yuan, F Xue, Y Yu, X Cao, Y Han, F Wang; (V) Data analysis and interpretation: X Yuan, F Xue, F Wang; (VI) Manuscript writing: All authors; (VII) Final approval of manuscript: All authors.

[#]These authors contributed equally to this work.

Correspondence to: Prof. Lou Zhong, MD; Fei Wang, MD. Department of Thoracic Surgery, Affiliated Hospital of Nantong University, No. 20 Xisi Road, Nantong 226001, China. Email: zhongl80@126.com; tdfywf@163.com.

Background: No effective drugs for the treatment of sepsis-induced diaphragm dysfunction are currently available. Therefore, it is particularly important to clarify the molecular regulatory mechanism of this condition and subsequently implement effective treatment and prevention of sepsis-induced diaphragm dysfunction.

Methods: A mouse model of diaphragm dysfunction was established via injection of lipopolysaccharide (LPS). An RNA-sequencing (RNA-seq) technique was used to detect the differentially expressed genes (DEGs) in the diaphragms of mice. Gene Ontology (GO) and Kyoto Encyclopedia of Genes and Genomes (KEGG) enrichment analyses were performed for functional analysis of DEGs. The protein-protein interaction network obtained from the Search Tool for the Retrieval of Interacting Genes/Proteins (STRING) website was imported into Cytoscape, the key molecular regulatory network was constructed with CytoNCA, the ClueGo plugin was further used to analyze the core regulatory pathways of key molecular, and finally, the iRegulon plugin was used to the identify key transcription factors.

Results: The genes upregulated after LPS treatment were involved in biological processes and pathways related to immune response; the genes downregulated after LPS treatment were mainly correlated with the muscle contraction. The expressions of several inflammation-related genes were upregulated after LPS treatment, of which tumor necrosis factor (*Tnf*), interleukin (*Il*)-*1β*, and *Il-6* assumed a core regulatory role in the network; meanwhile, the downregulated key genes included *Col1a1*, *Uqcrfs1*, *Sdhb*, and *ATP5a1*, among others. These key regulatory factors participated in the activation of Toll-like receptor (TLR) signaling pathway, nuclear factor (NF)-κB signaling pathway, and TNF signaling pathway as well as the inhibition of oxidative phosphorylation pathway, cardiac muscle contraction pathway, and citrate cycle pathway. Finally, RelA, IRF1, and STAT3, were identified as the key regulators in the early stage of diaphragmatic inflammatory response.

Conclusions: Sepsis-induced diaphragm dysfunction in mice is closely correlated with the activation of TLR signaling pathway, NF-κB signaling pathway, and TNF signaling pathway and the inhibition of oxidative phosphorylation pathway, cardiac muscle contraction pathway, and citrate cycle pathway. Our findings provide insight into the molecular mechanism of sepsis-induced diaphragm dysfunction in mice and provide a promising new strategy for targeted treatment of diaphragm dysfunction.

Keywords: Diaphragm dysfunction; sepsis; inflammation; energy metabolism

Submitted Nov 02, 2023. Accepted for publication Dec 13, 2023. Published online Dec 26, 2023.
doi: 10.21037/jtd-23-1680
View this article at: https://dx.doi.org/10.21037/jtd-23-1680

Introduction

The diaphragm is the most important respiratory muscle in the body, and normal respiratory functions are profoundly altered during general anesthesia, intra-thoracic or intra-abdominal surgery, and mechanical ventilation (1). Sepsis, a systemic inflammatory response syndrome caused by the invasion of pathogenic microorganisms such as bacteria, can lead to metabolic disorders, tissue damage, multiple organ dysfunction, and even death (2). It is reported that sepsis can rapidly lead to myopathy, resulting in dysfunction and atrophy of respiratory muscles and limb muscles (3,4). Patients with sepsis usually require intensive care treatment, and severe diaphragm dysfunction will prolong the mechanical ventilation time in critically ill patients, resulting in a longer intensive care unit stay and reducing the quality of life of patients after discharge (5). In addition, sepsis is a risk factor for the occurrence of acute respiratory distress syndrome (ARDS), which is associated with a higher mortality rate (6).

The maintenance of skeletal muscle homeostasis is critical to maintaining the normal structure and function of skeletal muscles (4,7-9). Continuous changes in the muscle microenvironment will disrupt the homeostasis of skeletal muscle, resulting in skeletal muscle dysfunction and atrophy (10-12). Some studies suggest that inflammation is one of the driving factors of skeletal muscle dysfunction and atrophy (13-15). Under inflammation, the levels of a large number of proinflammatory factors in the muscle of patients with sepsis, such as interleukin (IL)-6, are increased, and the binding of inflammatory factors to their receptors activates nuclear factor (NF)-κB, Janus kinase/signal transducer and activator of transcription (JAK/STAT), and p38 mitogen-activated protein kinase (MAPK) signaling pathways, thus leading to increased protein hydrolysis. In addition, the mitochondrial function of muscle cells is impaired, and reactive oxygen species (ROS) are produced in large quantities, resulting in oxidative stress damage and activation of excessive autophagy and, in turn, muscle dysfunction and atrophy (16-19). A study has found that levosimendan has been found protect from sepsis-inducing cardiac dysfunction by suppressing inflammation, oxidative stress and regulating cardiac mitophagy via the PINK-1-Parkin pathway in mice (20). Moreover, sepsis can trigger changes in the neuroendocrine system, such as the downregulation of insulin and insulin-like growth factor-1 (IGF-1) and damage to protein synthesis, which further lead to skeletal muscle damage (21).

Transcriptomic analysis was conducted in order to elucidate the molecular mechanism of sepsis-induced muscle injury. Thus far, the transcriptome sequencing of sepsis-induced muscle injury has mainly been conducted to study the mechanism of limb muscle atrophy (22,23). The reaction of skeletal muscle to sepsis varies according to the types of muscle fibers. The reaction of the diaphragm is different from that of limb muscles, as is the mechanism of injury (24). Moreover, the cause of diaphragm muscle weakness is likely to be complex. Therefore, this study conducted a transcriptomic analysis on sepsis-induced diaphragm dysfunction. Lipopolysaccharide (LPS) injection is one of the commonly used methods for establishing an experimental animal model of sepsis, and LPS can activate the signaling pathways to increase the degradation rate of muscle proteins (1,25). In this study, a mouse model of sepsis-induced diaphragm dysfunction was constructed with LPS injection; the differentially expressed genes (DEGs) in the diaphragms of mice at 24, 48, and 72 hours after LPS treatment were detected with RNA-sequencing (RNA-seq) technology, and the functions and key regulatory factors of the DEGs were analyzed. This study clarified the molecular mechanism of sepsis-induced diaphragm dysfunction, which can provide a target for the clinical treatment of septic

Highlight box

Key findings

- This study conducted a transcriptomic analysis on sepsis-induced diaphragm dysfunction. The result indicated that sepsis-induced diaphragm dysfunction is closely correlated with the activation of Toll-like receptor, nuclear factor-κB, and tumor necrosis factor signaling pathway and the inhibition of oxidative phosphorylation, cardiac muscle contraction, and citrate cycle pathway.

What is known and what is new?

- Patients with sepsis usually require intensive care treatment, and severe diaphragm dysfunction will prolong the mechanical ventilation time in critically ill patients. The causes of diaphragmatic weakness are very complex, and the underlying mechanism has not been fully understood.
- Here, we found pro-inflammatory signaling pathway were activated, while energy metabolism pathways were inhibited during sepsis induced diaphragm dysfunction.

What is the implication, and what should change now?

- This study clarified the molecular mechanism underlying diaphragm dysfunction in sepsis mice. Further study is needed to elucidate the cross-synergistic role of these key genes, and novel strategies based on the targeted treatment of diaphragm dysfunction should be actively developed.

myopathy, strengthen the respiratory system of patients, reduce the occurrence of ARDS, and improve the quality of life of patients. We present this article in accordance with the ARRIVE reporting checklist (available at https://jtd.amegroups.com/article/view/10.21037/jtd-23-1680/rc).

Methods

Experimental animal model

A total of 40 8-week-old Institute of Cancer Research (ICR) mice, weighing about 28 g, were provided from the Experimental Animal Center of Nantong University. The mice were raised in an air-conditioned room with a temperature of 21–25 ℃ and 55%±5% relative humidity and provided with sufficient water and food; a 24-hour circadian rhythm was maintained, with an equal day-time and night-time period. The animal experiment was conducted in accordance with Nantong University guidelines for the care and use of laboratory animals and was approved by the Animal Experiment Ethics Committee of Nantong University (No. S20200312-003). A protocol was prepared before the study without registration. The mice were randomly divided into a control group and an experimental group. The mice in the experimental group were injected intraperitoneally with LPS (0.4 mg/mL, 20 mg/kg) to establish mouse models of sepsis, while the mice in the control group received no treatment. The mice in the experimental group were anesthetized with bromethol (0.2 mL/10 g) at 24, 48, and 72 hours after LPS injection, and then the diaphragms in mice were harvested for subsequent experiments.

Histochemical staining

The diaphragm tissue was fixed in 4% formaldehyde and subjected to gradient dehydration with 10%, 20%, and 30% sucrose solution in sequence to prepare 12-μm-thick frozen sections. All sections underwent hematoxylin and eosin (HE) staining and sealing, and then the morphology of diaphragm was observed under a microscope.

Transcriptome sequencing analysis

A mirVana miRNA Isolation Kit (Thermo Fisher Scientific, Waltham, MA, USA) was used to extract RNA, and a NanoDrop 2000 (Thermo Fisher Scientific) was used for RNA quantification. According to the manufacturer's instructions, 1 μg of total RNA was extracted from each sample to construct a messenger RNA (mRNA) library using TruSeq Stranded Total RNA with Ribo-Zero Gold kits (Illumina, San Diego, CA, USA). A separation kit was used to digest ribosomal RNA and break it into short fragments. The first-strand complement DNA (cDNA) was synthesized using the broken RNA as a template, the second-strand synthesis reaction buffer was prepared to synthesize the second-strand cDNA, and the double-strand cDNA was purified and repaired at the end using a kit. The A tail was added, a sequencing joint was connected, and then the fragment size of the double-strand cDNA was determined. Finally, polymerase chain reaction (PCR) amplification was carried out. After the constructed library passed the quality inspection under an Agilent 2100 Bioanalyzer (Santa Clara, CA, USA), sequencing was conducted using the Illumina HiSeq™ 2500 or the Illumina HiSeq X Ten.

The raw reads obtained by sequencing were filtered using SortMeRNA and Trimmomatic software, while the quality of the clean reads was assessed using FastQC software. The comparison of reads was performed using HISAT2 software, while the results were analyzed using the RSeQC package. StringTie (v.2.0.3) was used to assemble transcripts based on genomic read alignments. After the clean reads were aligned to the transcription template using Bowtie2 software, the transcripts were quantified by eXpress software to obtain the fragments per kilobase of exon per million mapped fragments (FPKM) value and number of mRNAs. DESeq software was used to standardize the number of mRNAs in each sample, the fold change was calculated, and the test of significance for the difference in the number of reads was conducted using negative binomial (NB) distribution.

Gene function analysis

Gene Ontology (GO) enrichment analysis and Kyoto Encyclopedia of Genes and Genomes (KEGG) pathway enrichment analysis was respectively performed using R software (The R Foundation for Statistical Computing, Vienna, Austria) based on the hypergeometric distribution of OE Biotech Co., Ltd. (Shanghai, China; https://www.oebiotech.com). For GO and KEGG pathway analysis, a P value less than 0.05 was considered to indicate significant enrichment. The expression profile of each category of enrichment was displayed based on the expression value converted from the average z score as follows: $z\ score\ (x) = (x - \mu)/\delta$ (26,27).

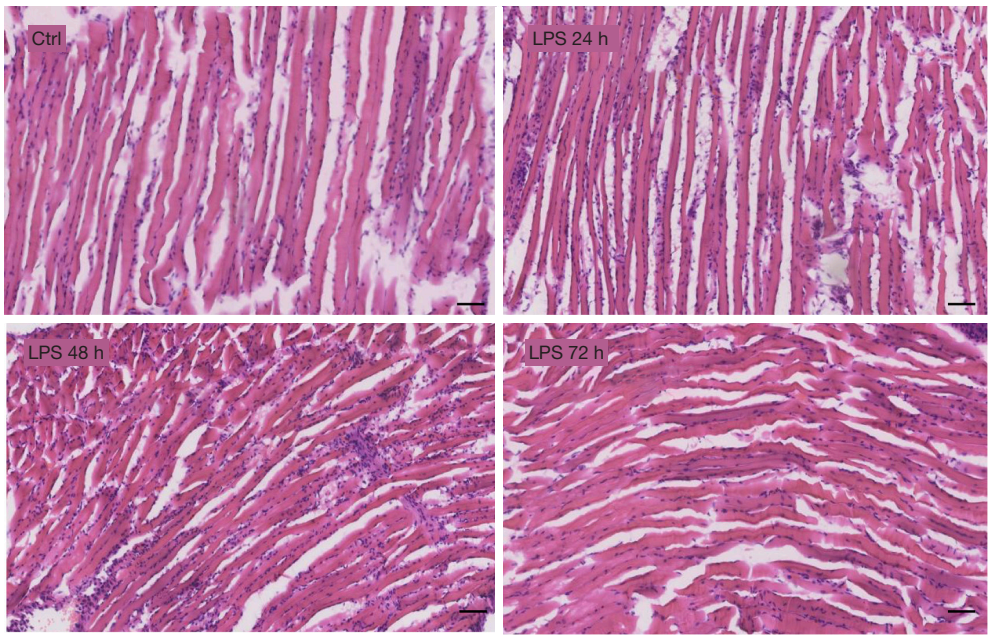

Figure 1 Changes in diaphragmatic structure after LPS treatment. Bar =50 μm. 12-μm thick frozen sections of diaphragm tissue were stained with HE. Ctrl, control; LPS, lipopolysaccharide; HE, hematoxylin and eosin.

Construction and analysis of a regulatory network

The Search Tool for the Retrieval of Interacting Genes/Proteins (STRING; https://cn.string-db.org/) was used to build an interactive network, with an interaction score ≥0.4. The results of interaction were downloaded and imported into the Cytoscape v.3.8.2 software. The CytoNCA plugin (sorted by degree) was used to further study the core regulatory network, the ClueGO plugin was used to identify the pathways involved in the subnetwork, and the iRegulon plugin was used to identify key transcription factors.

Statistical analysis

In the RNA-seq data, a P value less than 0.05 and a fold change greater than two indicated there to be a differential expression of the same gene between the two samples.

Results

Diaphragm dysfunction caused by LPS treatment

The diaphragmatic muscle from the mice was stained with HE to observe the morphological changes in the diaphragmatic muscle in sepsis mice. Compared with that in the control group, the longitudinal section of the diaphragmatic muscle from the mice treated with LPS was irregular, the distance between muscle fibers was elongated, and the infiltration of inflammatory cells was increased at 24 hours after LPS treatment (*Figure 1*). The above results show that the mouse model of sepsis-induced diaphragm dysfunction was successfully constructed with LPS in this study.

Effect of LPS treatment on gene expression in the diaphragm

In order to clarify the regulatory mechanism of diaphragmatic atrophy caused by sepsis, RNA was extracted from the diaphragms in the normal control group and those at different time points after LPS treatment for transcriptome sequencing analysis. Principal component analysis (PCA) showed the significant changes in gene expression in the diaphragm after LPS treatment, with a good intragroup homogeneity (*Figure 2A*). Compared with the control group, the experimental group had 914 upregulated genes and 1,521 downregulated genes at 24 hours after LPS treatment, 1,221 upregulated genes and 865 downregulated genes at 48 hours, and 1,518 upregulated genes and 1,009 downregulated genes (*Figure 2B*) at 72 hours. The differential gene expression heatmaps are

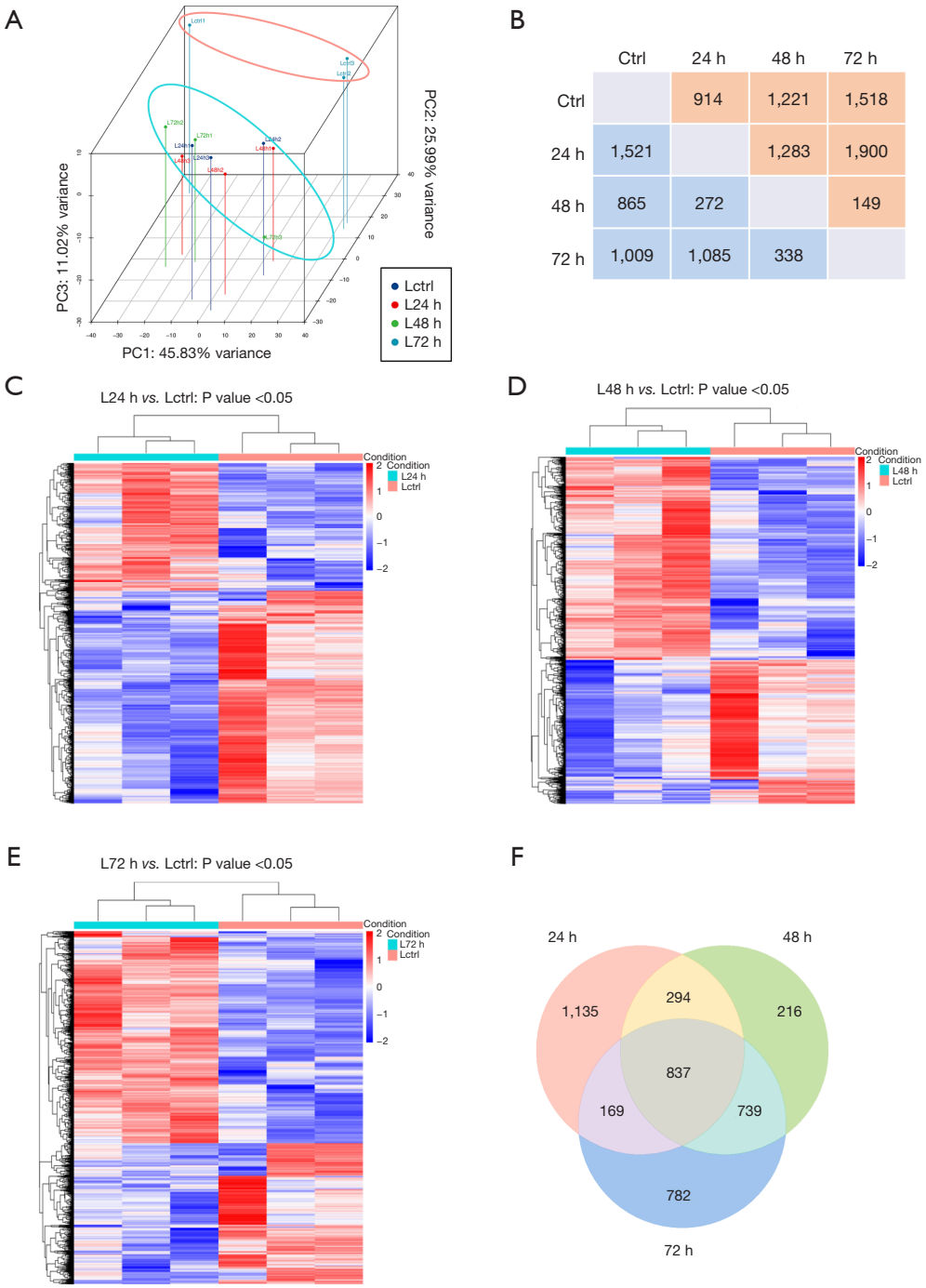

Figure 2 Analysis of DEGs in the mouse diaphragm after LPS treatment. (A) PCA analysis. (B) Comparison of the number of DEGs in the mouse diaphragm of the LPS-treatment and control group at different time points after treatment. (C-E) Differential gene expression heatmaps at different time points after LPS treatment. (F) Venn diagram analysis of the number of differentially co-expressed genes at different time points after LPS treatment. PC, principal component; ctrl, control; DEG, differentially expressed gene; LPS, lipopolysaccharide; PCA, principal component analysis.

shown in the *Figure 2C-2E*. Venn diagram analysis showed that a total of 837 genes were differentially expressed at 3-time points after LPS treatment, and the number of differentially co-expressed genes was greater at 48 and 72 hours after LPS treatment (*Figure 2F*).

Functional analysis of DEGs in the diaphragm regulated with LPS treatment

In order to analyze the functions of these DEGs, we conducted GO and KEGG enrichment analyses on DEGs at different time points after LPS treatment. GO analysis showed that the genes upregulated after LPS treatment were mainly involved in the biological processes related to immune response and inflammatory response, and the genes upregulated at 48–72 hours after LPS treatment also participated in the biological processes related to cell cycle (*Figure 3A*). The KEGG enrichment analysis showed that the genes upregulated after LPS treatment were mainly involved in the tumor necrosis factor (TNF) signaling pathway, cytokine-cytokine receptor interaction, nucleotide oligomerization domain (NOD)-like receptor signaling pathway, NF-κB signaling pathway, phagosome, and natural killer (NK) cell-mediated cytotoxicity pathways, all of which contribute to inflammation. Furthermore, the genes upregulated at 48–72 hours after LPS treatment also participated in the cell cycle-related pathway (*Figure 3B*).

GO analysis showed that the genes downregulated at 24 hours after LPS treatment were involved in biological processes such as cell adhesion and muscle contraction, and the genes downregulated at 48–72 hours after LPS treatment were involved in biological processes such as muscle contraction, energy metabolism in mitochondrial respiratory chain, and fatty-acid metabolism (*Figure 4A*). KEGG enrichment analysis showed that the genes downregulated after LPS treatment were mainly involved in energy-producing pathways such as cardiac contraction, pyruvate metabolism, and citric acid cycle; the genes downregulated at 24 hours after LPS treatment also participating in adhesion, protein digestion and absorption, and PI3K-AKT signaling pathways; the genes downregulated at 48–72 hours after LPS treatment also participated in oxidative phosphorylation pathway (*Figure 4B*). The above results suggest that the immune response was significantly activated and energy metabolism inhibited in the diaphragms of sepsis mice.

Analysis of key genes and pathways in diaphragm dysfunction after LPS treatment

In order to identify the key DEGs in diaphragms of the sepsis mice, a protein interaction network obtained from the STRING website was imported into Cytoscape and analyzed with the CytoNCA plugin. At 24–72 hours after LPS treatment, upregulation was observed in inflammatory genes such as *Tnf*, ILs such as *Il-1β*, *Il-6*, and *Il-10*; Toll-like receptors (TLRs) such as *Tlr2* and *Tlr4*; and inflammatory factors such as *Ccl5* and *Itgam*. Of these, TNF, IL-1β, and IL-6 played a core regulatory role in the network. In addition, the key genes upregulated at 24 hours after LPS treatment also included multiple transcription factors such as Irf1/7 and Stat1/3, as well as inflammatory-related factors such as Csf2, Cxcl9, and Cxcl10. The key genes upregulated at 48–72 hours after LPS treatment also included *Ptprc*, *Syk* related to immune response, and *Mki67*, *Ccnb1*, and *Plk1* related to cell cycle (*Figure 5A-5C*). The heat map of the expression levels of these key DEGs is shown in *Figure 5D*. The key genes upregulated at 24–72 hours after LPS treatment were mainly involved in inflammation-related pathways, such as TLR signaling pathway, NF-κB signaling pathway, and TNF signaling pathway. These pathways were significantly activated at 24 hours after LPS treatment (*Figure 6*).

At 24 hours after LPS treatment, the expression levels of several genes encoding extracellular matrix (ECM) were downregulated, including the genes encoding collagen such as *Col1a1*, *Fras1*, *Itgb5*, and *Acan*. The downregulated genes also included *Acta2*, *Actn2*, and *Bdnf* (*Figure 7A*). The key genes downregulated at 48–72 hours after LPS treatment were approximately the same, including multiple genes encoding complex proteins involved in mitochondrial oxidative phosphorylation, such as *Uqcrfs1*, *Sdhb*, and *Cyc1*, as well as those involved in adenosine triphosphate (ATP) synthetases such as *Atp5a1* and *Atp5o* (*Figure 7B*,*7C*). The heat map of the expression levels of these key DEGs is shown in *Figure 7D*. The key genes downregulated at 24 hours after LPS treatment were mainly involved in ECM-receiver interaction and protein digestion and absorption pathways (*Figure 8A*). The key genes downregulated at 48–72 hours after LPS treatment were mainly involved in oxidative phosphorylation, cardiac muscle contract pathways, etc.; of these, the key genes downregulated at 72 hours after LPS treatment were also involved in the

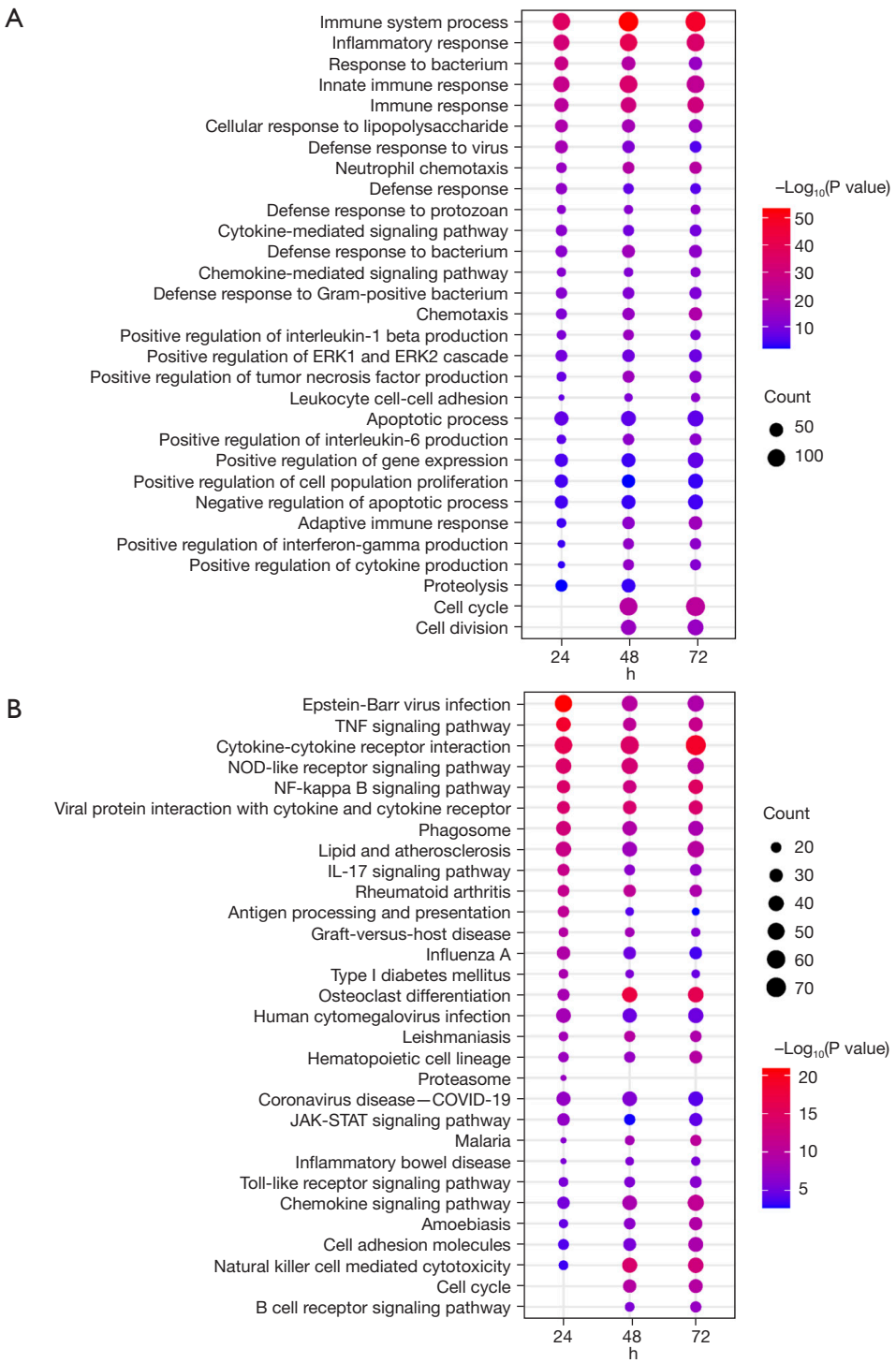

Figure 3 Functional analysis of DEGs in the diaphragm upregulated after LPS treatment. (A) GO biological process enriched by the genes upregulated at different time points. (B) KEGG enrichment analysis of genes upregulated at different time points. The circle's size and color indicate the number and $-\log_{10}$(P value) of DEGs annotated in the specific terms, respectively. ERK, extraneous signal-regulated kinase; TNF, tumor necrosis factor; NOD, nucleotide oligomerization domain; NF, nuclear factor; IL, interleukin; COVID-19, coronavirus disease 2019; JAK-STAT, Janus kinase-signal transducer and activator of transcription; DEG, differentially expressed gene; LPS, lipopolysaccharide; GO, Gene Ontology; KEGG, Kyoto Encyclopedia of Genes and Genomes.

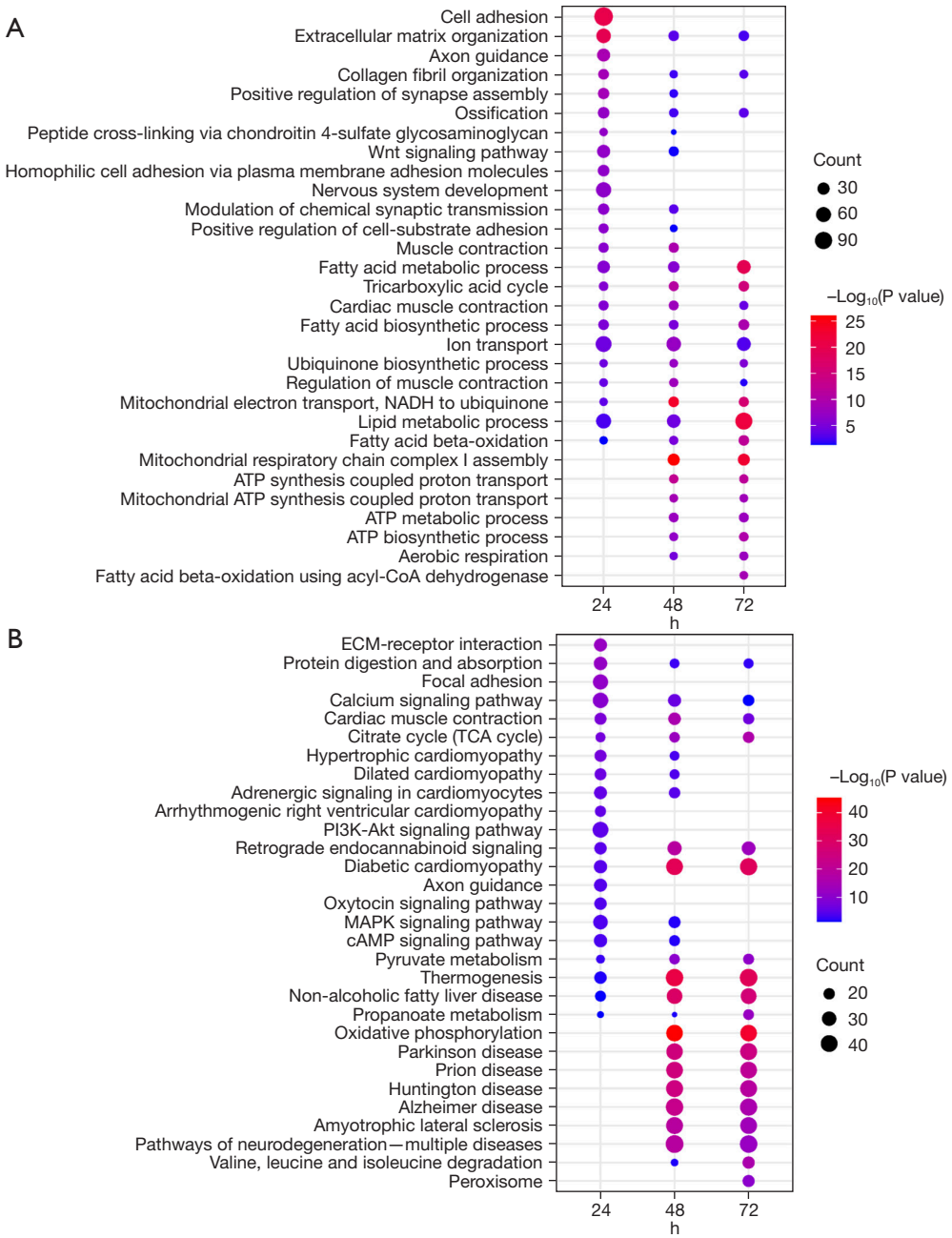

Figure 4 Functional analysis of the DEGs in the diaphragm downregulated after LPS treatment. (A) The GO biological processes enriched by the genes downregulated at different time points. (B) KEGG enrichment analysis of genes downregulated at different time points. The circle's size and color indicate the number and $-\log_{10}$(P value) of DEGs annotated in the specific terms, respectively. NADH, reduced forms of the nicotinamide adenine dinucleotide; ATP, adenosine triphosphate; CoA, coenzyme A; ECM, extracellular matrix; TCA, tricarboxylic acid; MAPK, mitogen-activated protein kinase; cAMP, cyclic adenosine monophosphate; DEG, differentially expressed gene; LPS, lipopolysaccharide; GO, Gene Ontology; KEGG, Kyoto Encyclopedia of Genes and Genomes.

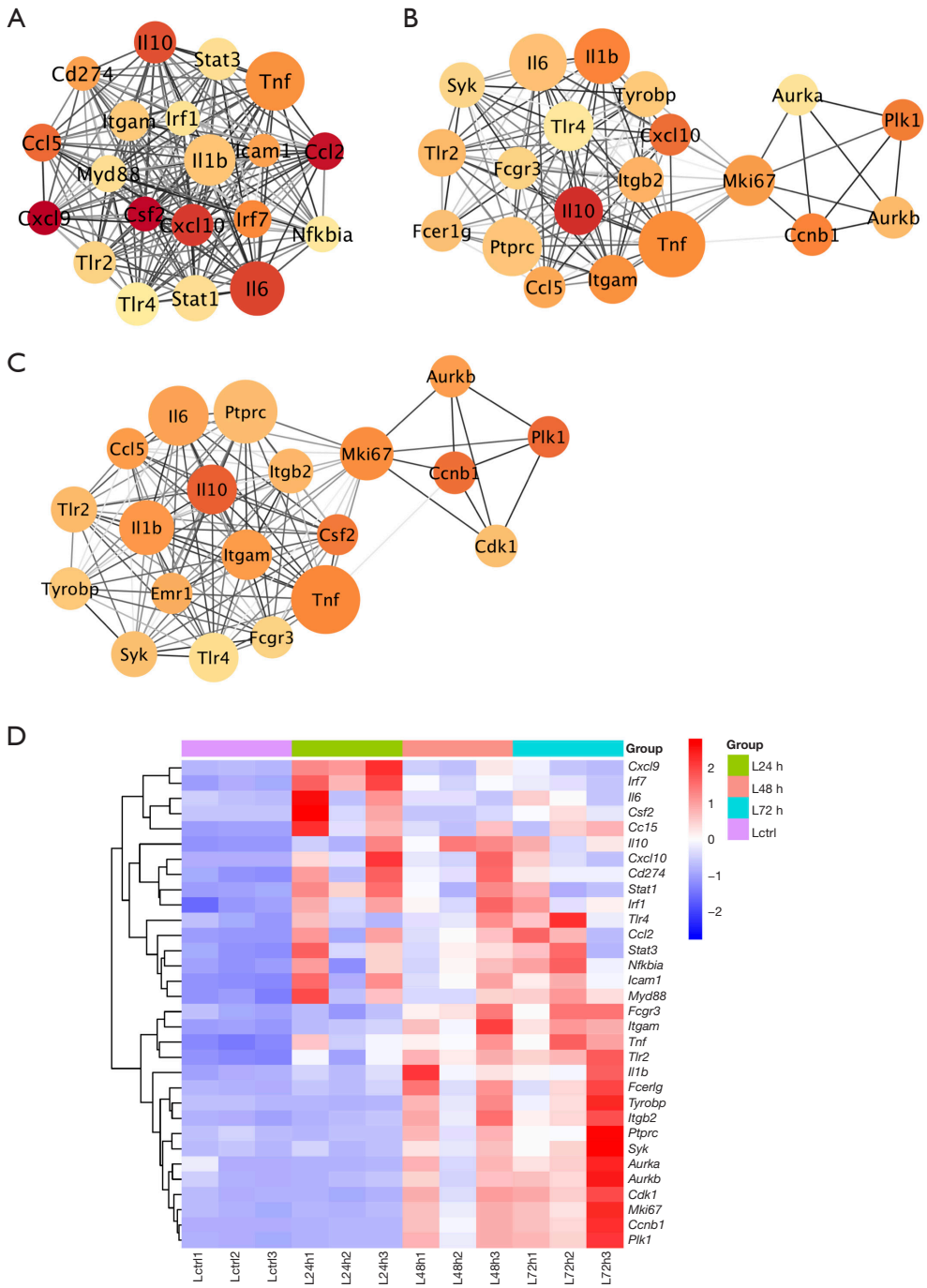

Figure 5 Analysis of key genes upregulated in the diaphragm at different time points after LPS treatment. (A) Analysis of key genes in the diaphragm at 24 h after LPS treatment. (B) Analysis of key genes in the diaphragm at 48 h after LPS treatment. (C) Analysis of key genes in the diaphragm at 72 h after LPS treatment. (D) A heat map of the expression levels of key genes upregulated in diaphragm at different time points after LPS treatment. The circle's size and color indicate the degree and fold of DEGs, respectively. Ctrl, control; LPS, lipopolysaccharide; DEG, differentially expressed gene.

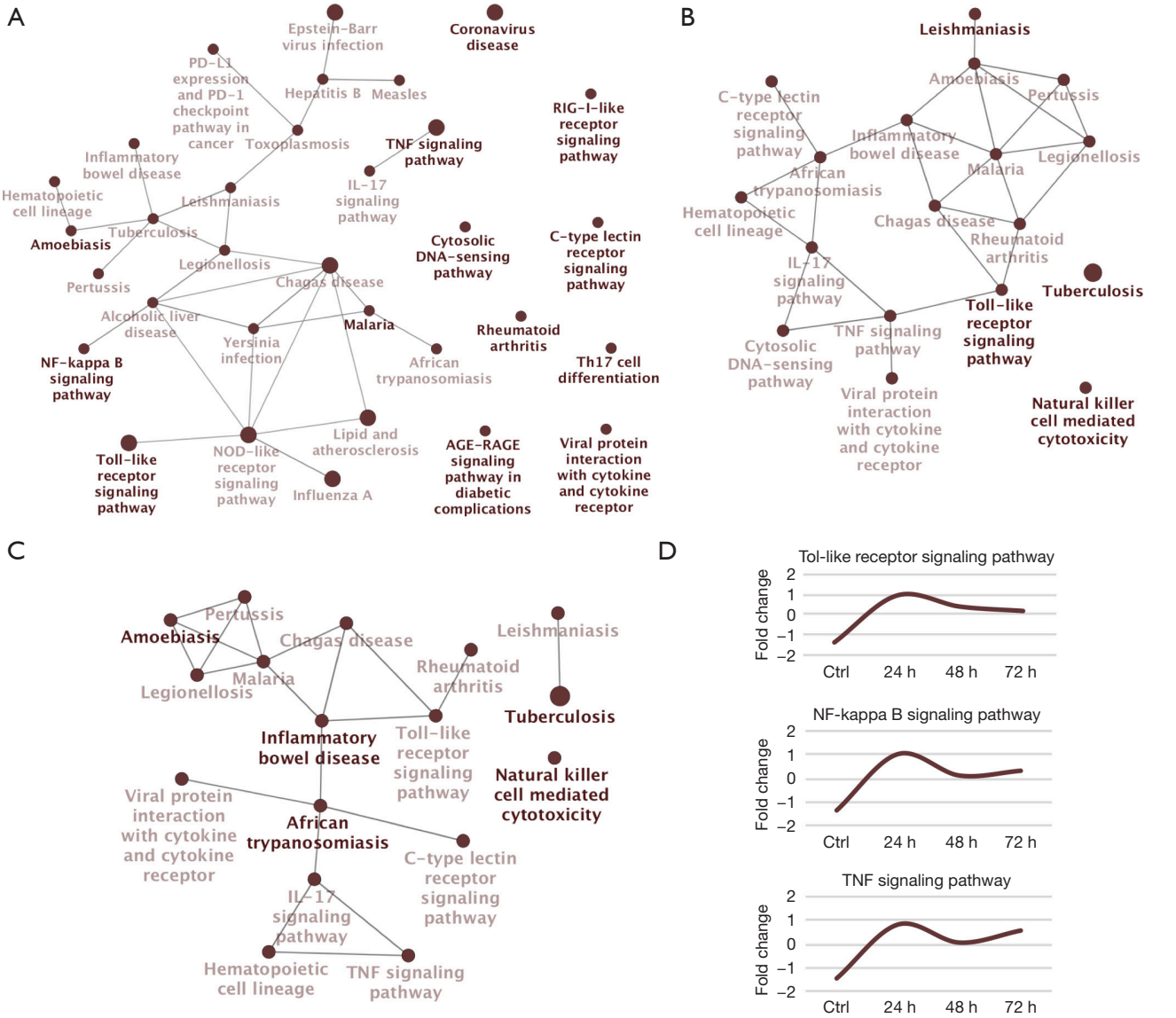

Figure 6 Analysis of key pathways upregulated in the diaphragm at different time points after LPS treatment. (A) Analysis of key pathways upregulated in the diaphragm at 24 h after LPS treatment. (B) Analysis of key pathways upregulated in the diaphragm at 48 h after LPS treatment. (C) Analysis of key pathways upregulated in diaphragm at 72 h after LPS treatment. (D) The average expression profiles of DEGs involved in the major KEGG pathways. The circle's size indicates the number of DEGs annotated in the given terms. PD-L1, programmed cell death ligand 1; PD-1, programmed cell death protein 1; TNF, tumor necrosis factor; IL, interleukin; NF, nuclear factor; NOD, nucleotide oligomerization domain; AGE, advanced glycation end products; RAGE, receptor for advanced glycation end products; ctrl, control; LPS, lipopolysaccharide; DEG, differentially expressed gene; KEGG, Kyoto Encyclopedia of Genes and Genomes.

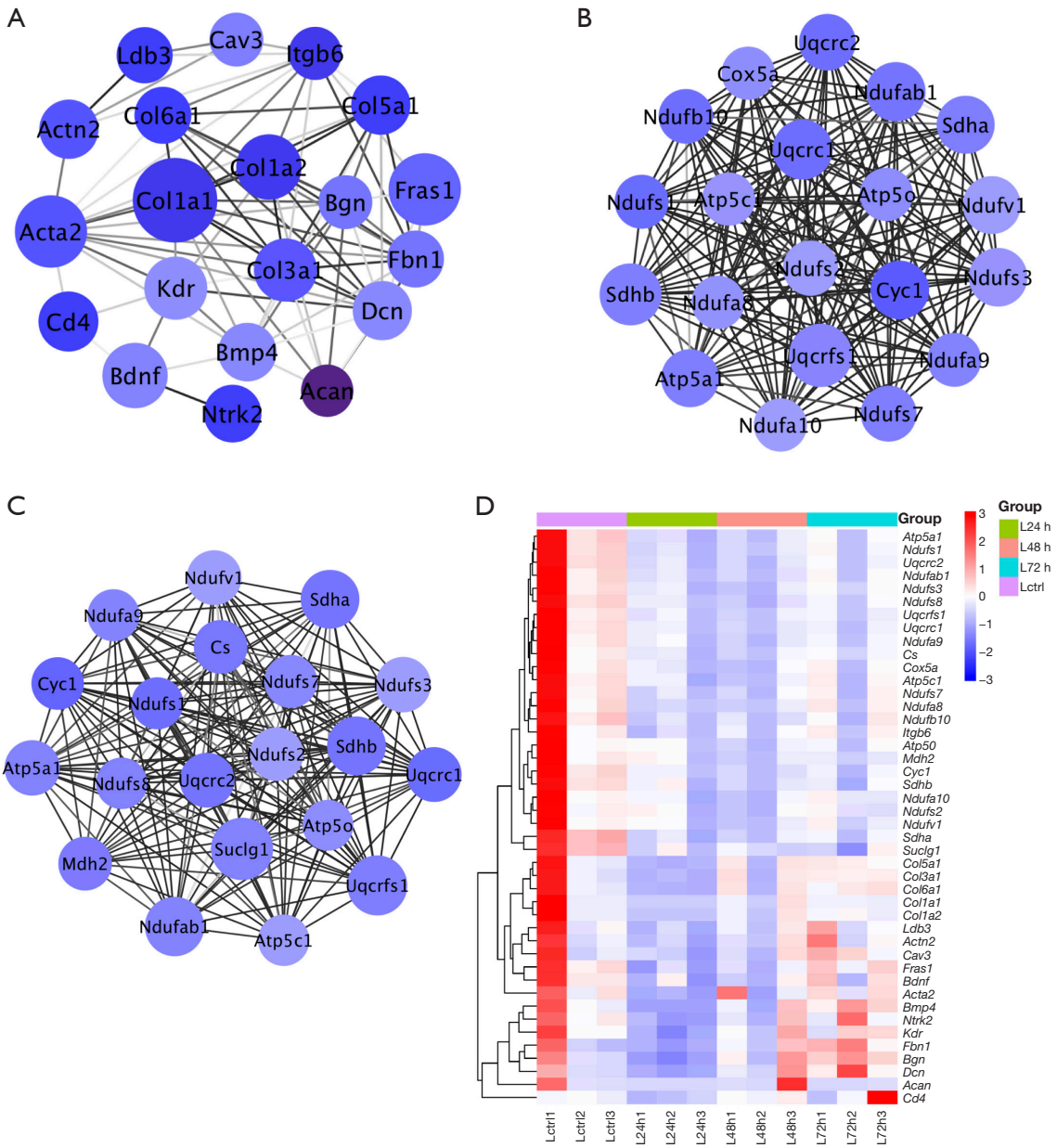

Figure 7 Analysis of key genes downregulated in diaphragm at different time points after LPS treatment. (A) Analysis of key genes downregulated in the diaphragm at 24 h after LPS treatment. (B) Analysis of key genes downregulated in diaphragm at 48 h after LPS treatment. (C) Analysis of key genes downregulated in diaphragm at 72 h after LPS treatment. (D) A heat map of key genes downregulated in the diaphragm at different time points after LPS treatment. The circle's size and color indicate the degree and fold change of DEGs, respectively. Ctrl, control; LPS, lipopolysaccharide; DEG, differentially expressed gene.

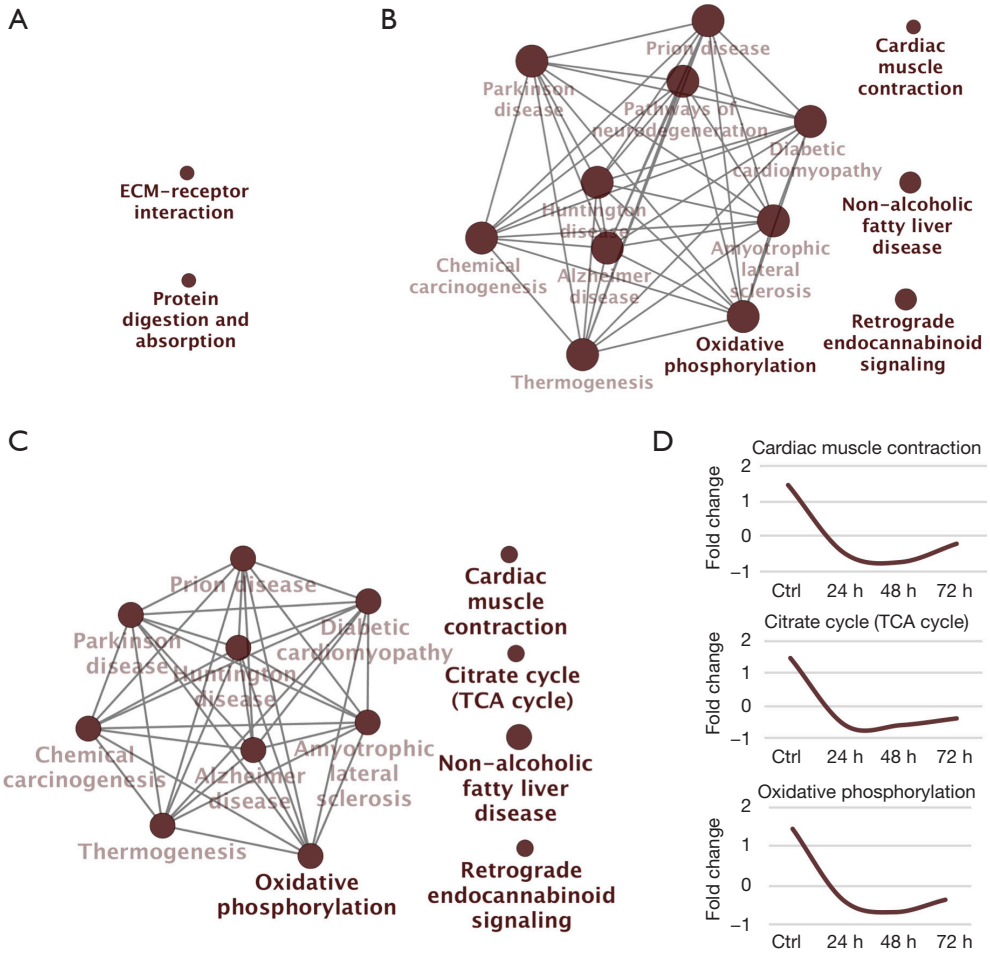

Figure 8 Analysis of the key pathways downregulated in the diaphragm at different time points after LPS treatment. (A) Analysis of key pathways downregulated in the diaphragm at 24 h after LPS treatment. (B) Analysis of key pathways downregulated in the diaphragm at 48 h after LPS treatment. (C) Analysis of key pathways downregulated in the diaphragm at 72 h after LPS treatment. (D) The average expression profiles of DEGs involved in major KEGG pathways. The circle's size indicates the number of DEGs annotated in the given terms. ECM, extracellular matrix; TCA, tricarboxylic acid; ctrl, control; LPS, lipopolysaccharide; DEG, differentially expressed gene; KEGG, Kyoto Encyclopedia of Genes and Genomes.

citrate cycle pathway, among others. These pathways were significantly inhibited at 24 hours after LPS treatment and gradually recovered at 72 hours after LPS treatment (*Figure 8B-8D*).

Transcription factor analysis of diaphragm dysfunction caused by LPS treatment

Finally, the iRegulon plugin was further used to analyze the transcription factors of key DEGs at 24 hours after LPS treatment. The results showed that the transcription factor RelA regulated 17 of the most critical molecules, including *Icam1* and *Ccl5* (*Figure 9A*). Other transcription factors included IRF1 and STAT3, which regulated 14 and 15 key molecules, respectively (*Figure 9B,9C*). Three transcription factors, RelA, IRF1, and STAT3, may have key roles in the diaphragm dysfunction of sepsis mice.

Discussion

Sepsis is a complex disease caused by a variety of microorganisms (usually bacteria) and a dysregulated host response to infection, with respiratory muscle injury being common in critically ill patients with sepsis. The diaphragm

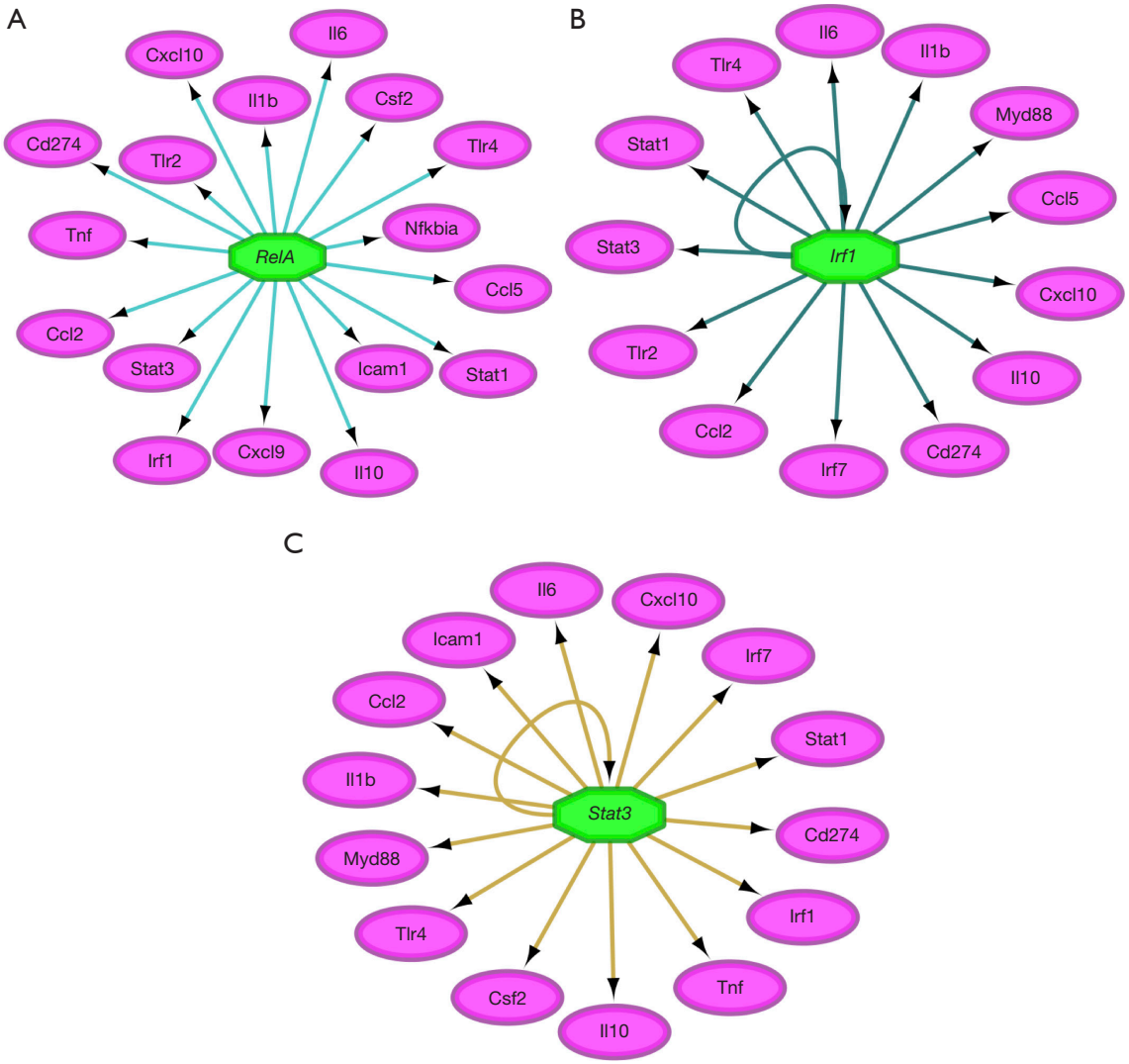

Figure 9 Analysis of key transcription factors at 24 h after LPS treatment. (A) Network of the key molecules regulated by *RelA*. (B) Network of the key molecules regulated by *Irf1*. (C) Network of the key molecules regulated by *Stat3*. LPS, lipopolysaccharide.

is a respiratory muscle composed of a continuously active skeletal muscle formed by almost equal amounts of type I and type II fibers. In this study, LPS injection was performed to establish a mouse model of sepsis, and it was found that after LPS treatment, the structures of the diaphragm muscle fibers were damaged, with inflammatory cell infiltration being observed. On this basis, the transcriptome analysis of DEGs in the diaphragm was performed at different time points after LPS treatment.

First, the expression levels of DEGs in the diaphragm at 24, 48, and 72 hours after LPS treatment were analyzed. After LPS treatment, the expression levels of a large number of genes in the diaphragm changed. The functional analyses of DEGs at different time points showed that the genes upregulated by LPS treatment were mainly correlated with immune response and inflammation. Inflammation plays an important role in regulating skeletal muscle injury and atrophy caused by various diseases, such as cancer, diabetes, and chronic kidney disease (8,28-30). Dysfunction of the diaphragm induced by sepsis has been found to increase the muscle's exposure to pro-inflammatory cytokines. Alleviation of sepsis-induced diaphragm dysfunction can be achieved by attenuating inflammation, for example, with $MgSO_4$ (31). Transcription factor analysis showed that most of the key molecules were regulated by the transcription factor RelA at 24 hours after LPS treatment. RelA can

encode the NF-κB p65 subunit to form a heterodimer with p50, which is a functional component involved in nuclear translocation and activation of NF-κB. NF-κB is one of the most important signaling molecules activated during skeletal muscle injury (15). LPS can induce skeletal muscle atrophy by increasing the activity of NF-κB and its downstream inflammatory mediators (such as TNF-α and IL-1β) to upregulate the expressions of MAFbx and MuRF1, while triptolide pretreatment can reduce LPS-induced skeletal muscle atrophy in limbs by inhibiting the NF-κB/TNF-α pathway (28). H_2S can improve LPS-induced diaphragm dysfunction in rats, regulate ROS/MAPK and TLR4/NF-κB signaling pathway, and reduce cell apoptosis, which is associated with inflammation (32). Our study further showed that NF-κB signaling pathway plays a key role in LPS-induced diaphragm dysfunction. Our previous study revealed that the infusion of IL-6 into the muscles of mice can induce skeletal muscle atrophy through the activation of immune receptors and the reduction of energy metabolism (14). Interfering with the activation of the JAK/STAT3 signaling pathway downstream of IL-6 can inhibit the denervation-induced activation of muscle ubiquitin proteasome and mitochondrial autophagy, thus alleviating denervation-induced skeletal muscle atrophy (19). A recent study reported that IL-6 acted on muscle cells via the gp130 and IL-6Rα complexes in the limb muscles of sepsis mice after cecal ligation and puncture, thus activating JAK2 and STAT3 signaling pathway. This subsequently led to the increased expression of SOCS3, the inhibition of IRS-1/Akt pathway, the decrease of protein synthesis, and enhanced protein degradation, ultimately mediating muscle atrophy (22). In this study, we analyzed the key molecules at each time point and found that IL-6, TNF, and IL-1β played a central regulatory role in the network. IL-6 (fold change =23.71) expression in diaphragm tissue increased sharply at 24 hours after LPS treatment. Later, when analyzing the key regulatory molecules at 24 hours after LPS treatment, we found that multiple molecules were regulated by the transcription factor STAT3, and the expression levels of STAT3 and SOCS3 downstream were also upregulated in the diaphragms of sepsis mice. A previous study indicated that JAK/STAT3 signaling plays an important role in the progression of diaphragm dysfunction during controlled mechanical ventilation (33). Therefore, we speculated that the IL-6-STAT3 axis may play a key role in respiratory muscle dysfunction in sepsis mice. In addition, the genes upregulated at 48–72 hours after LPS treatment were also related to cell cycle, which may be correlated with the proliferation of muscle satellite cells or immune cells; this, relationship should be further investigated with further detection and analysis.

The key genes downregulated after LPS treatment were mainly related to muscle contraction, suggesting diaphragm dysfunction was present in sepsis mice. The key genes downregulated at 24 hours after LPS treatment also included multiple genes, including *Col1a1*, which is related to cell adhesion. *Col1a1* encodes type I collagen α1 chain, and its mutation is often associated with osteogenesis imperfecta (34). Type I collagen is expressed in the skeletal muscles during development and in adult muscle tissues. A recent study indicated that the mass and contractility of the diaphragm decreased in the mouse model with osteogenesis imperfecta caused by *Col1a1* mutation (35). In our study, the genes downregulated at 48–72 hours after LPS treatment, including Uqcrfs1, Sdhb, and ATP5a1, participate in the pathways related to mitochondrial energy metabolism, such as the oxidative phosphorylation and citrate cycle pathways. Mitochondria are the key organelles responsible for regulating the metabolic state of skeletal muscles. A recent study showed that in a mouse muscle injury model with intramuscular adipose tissue (IMAT) infiltration, GADD45A regulated fat infiltration and mitochondrial function via binding to mitochondrial complex protein ATP5A1 to promote its degradation, thus leading to the reduction of ATP and the inactivation of the cAMP/PKA/LKB1 signaling pathway (36). Sepsis-induced muscle weakness may also be correlated with the excessive generation of mitochondrial free radicals and mitochondrial autophagy (37-39). A study indicates that cytokine-activated skeletal muscle calcium-dependent phospholipase A2 is connected with mitochondrial superoxide generation. The activation of calpain in the diaphragm as a consequence of infection can be attenuated by therapies that scavenge mitochondrial superoxide radicals and/or inhibit cPLA2, therefore preventing the development of diaphragm weakness in infected individuals (40). Another study has shown that when MitoTEMPOL, an agent targeted at mitochondria, is administered, it can prevent reductions in diaphragm force generation and diaphragm mitochondrial function induced by sepsis (37). Therefore, there is potential for translation of agents with antioxidant properties into clinical trials, which may help preserve diaphragm function and improve clinical outcomes in critically ill patients.

Conclusions

In conclusion, this study demonstrated that the expression levels of inflammatory cytokines such as TNF, IL-1β, and IL-6 in the diaphragms of sepsis mice are upregulated; moreover, TLR signaling pathway and rapid activation of related pathways such as NF-κB signaling pathway and TNF signaling pathway, along with the activation of transcription factors such as RelA, IRF1, and STAT3, exert a crucial regulatory role in diaphragm dysfunction. Meanwhile, energy metabolism pathways such as cardiac muscle contraction, oxidative phosphorylation, and citrate cycle were inhibited. This study clarified the molecular mechanism underlying diaphragm dysfunction in sepsis mice; nonetheless, further study is needed to fully understand and elucidate the cross-synergistic role of these key genes and pathways in the process of diaphragm dysfunction in mice, and novel strategies based on the targeted treatment of diaphragm dysfunction should be actively developed.

Acknowledgments

We thank Dr. Willem N. Welvaart (Department of General Thoracic Surgery and Oncology, Meander Medical Center, Amersfoort, the Netherlands) for the critical comments and valuable advice on this study.

Funding: This work was supported by the Natural Science Research Project of Nantong Science and Technology Bureau (No. MS12020029).

Footnote

Reporting Checklist: The authors have completed the ARRIVE reporting checklist. Available at https://jtd.amegroups.com/article/view/10.21037/jtd-23-1680/rc

Data Sharing Statement: Available at https://jtd.amegroups.com/article/view/10.21037/jtd-23-1680/dss

Peer Review File: Available at https://jtd.amegroups.com/article/view/10.21037/jtd-23-1680/prf

Conflicts of Interest: All authors have completed the ICMJE uniform disclosure form (available at https://jtd.amegroups.com/article/view/10.21037/jtd-23-1680/coif). The authors have no conflicts of interest to declare.

Ethical Statement: The authors are accountable for all aspects of the work in ensuring that questions related to the accuracy or integrity of any part of the work are appropriately investigated and resolved. Animal experiments were performed under a project license (No. S20200312-003) granted by Animal Protection and Utilization Committee of Nantong University, in compliance with Nantong University guidelines for the care and use of animals.

References

1. Oliveira TS, Santos AT, Andrade CBV, et al. Sepsis Disrupts Mitochondrial Function and Diaphragm Morphology. Front Physiol 2021;12:704044.
2. Lelubre C, Vincent JL. Mechanisms and treatment of organ failure in sepsis. Nat Rev Nephrol 2018;14:417-27.
3. Baldwin CE, Bersten AD. Alterations in respiratory and limb muscle strength and size in patients with sepsis who are mechanically ventilated. Phys Ther 2014;94:68-82.
4. Wang W, Shen D, Zhang L, et al. SKP-SC-EVs Mitigate Denervated Muscle Atrophy by Inhibiting Oxidative Stress and Inflammation and Improving Microcirculation. Antioxidants (Basel) 2021;11:66.
5. Petrof BJ. Diaphragm Weakness in the Critically Ill: Basic Mechanisms Reveal Therapeutic Opportunities. Chest 2018;154:1395-403.
6. Supinski GS, Morris PE, Dhar S, et al. Diaphragm Dysfunction in Critical Illness. Chest 2018;153:1040-51.
7. Zhang L, Li M, Wang W, et al. Celecoxib alleviates denervation-induced muscle atrophy by suppressing inflammation and oxidative stress and improving microcirculation. Biochem Pharmacol 2022;203:115186.
8. Shen Y, Li M, Wang K, et al. Diabetic Muscular Atrophy: Molecular Mechanisms and Promising Therapies. Front Endocrinol (Lausanne) 2022;13:917113.

9. Huang L, Li M, Deng C, et al. Potential Therapeutic Strategies for Skeletal Muscle Atrophy. Antioxidants (Basel) 2022;12:44.
10. Gan Z, Fu T, Kelly DP, et al. Skeletal muscle mitochondrial remodeling in exercise and diseases. Cell Res 2018;28:969-80.
11. Chen W, You W, Valencak TG, et al. Bidirectional roles of skeletal muscle fibro-adipogenic progenitors in homeostasis and disease. Ageing Res Rev 2022;80:101682.
12. Wang W, Li M, Chen Z, et al. Biogenesis and function of extracellular vesicles in pathophysiological processes of skeletal muscle atrophy. Biochem Pharmacol 2022;198:114954.
13. Crossland H, Constantin-Teodosiu D, Greenhaff PL. The Regulatory Roles of PPARs in Skeletal Muscle Fuel Metabolism and Inflammation: Impact of PPAR Agonism on Muscle in Chronic Disease, Contraction and Sepsis. Int J Mol Sci 2021;22:9775.
14. Sun H, Sun J, Li M, et al. Transcriptome Analysis of Immune Receptor Activation and Energy Metabolism Reduction as the Underlying Mechanisms in Interleukin-6-Induced Skeletal Muscle Atrophy. Front Immunol 2021;12:730070.
15. Ji Y, Li M, Chang M, et al. Inflammation: Roles in Skeletal Muscle Atrophy. Antioxidants (Basel) 2022;11:1686.
16. Cao YY, Wang Z, Yu T, et al. Sepsis induces muscle atrophy by inhibiting proliferation and promoting apoptosis via PLK1-AKT signalling. J Cell Mol Med 2021;25:9724-39.
17. Wan Q, Zhang L, Huang Z, et al. Aspirin alleviates denervation-induced muscle atrophy via regulating the Sirt1/PGC-1α axis and STAT3 signaling. Ann Transl Med 2020;8:1524.
18. Shen Y, Zhang Q, Huang Z, et al. Isoquercitrin Delays Denervated Soleus Muscle Atrophy by Inhibiting Oxidative Stress and Inflammation. Front Physiol 2020;11:988.
19. Huang Z, Zhong L, Zhu J, et al. Inhibition of IL-6/JAK/STAT3 pathway rescues denervation-induced skeletal muscle atrophy. Ann Transl Med 2020;8:1681.
20. Shi J, Chen Y, Zhi H, et al. Levosimendan protects from sepsis-inducing cardiac dysfunction by suppressing inflammation, oxidative stress and regulating cardiac mitophagy via the PINK-1-Parkin pathway in mice. Ann Transl Med 2022;10:212.
21. Martín AI, Priego T, López-Calderón A. Hormones and Muscle Atrophy. Adv Exp Med Biol 2018;1088:207-33.
22. Zanders L, Kny M, Hahn A, et al. Sepsis induces interleukin 6, gp130/JAK2/STAT3, and muscle wasting. J Cachexia Sarcopenia Muscle 2022;13:713-27.
23. Cho DS, Schmitt RE, Dasgupta A, et al. Single-cell deconstruction of post-sepsis skeletal muscle and adipose tissue microenvironments. J Cachexia Sarcopenia Muscle 2020;11:1351-63.
24. Moreno-Rupérez Á, Priego T, González-Nicolás MÁ, et al. Role of Glucocorticoid Signaling and HDAC4 Activation in Diaphragm and Gastrocnemius Proteolytic Activity in Septic Rats. Int J Mol Sci 2022;23:3641.
25. Ono Y, Maejima Y, Saito M, et al. TAK-242, a specific inhibitor of Toll-like receptor 4 signalling, prevents endotoxemia-induced skeletal muscle wasting in mice. Sci Rep 2020;10:694.
26. Shen Y, Zhang R, Xu L, et al. Microarray Analysis of Gene Expression Provides New Insights Into Denervation-Induced Skeletal Muscle Atrophy. Front Physiol 2019;10:1298.
27. Parikh JR, Klinger B, Xia Y, et al. Discovering causal signaling pathways through gene-expression patterns. Nucleic Acids Res 2010;38:W109-17.
28. Fang WY, Tseng YT, Lee TY, et al. Triptolide prevents LPS-induced skeletal muscle atrophy via inhibiting NF-κB/TNF-α and regulating protein synthesis/degradation pathway. Br J Pharmacol 2021;178:2998-3016.
29. Chiappalupi S, Sorci G, Vukasinovic A, et al. Targeting RAGE prevents muscle wasting and prolongs survival in cancer cachexia. J Cachexia Sarcopenia Muscle 2020;11:929-46.
30. Wang K, Liu Q, Tang M, et al. Chronic kidney disease-induced muscle atrophy: Molecular mechanisms and promising therapies. Biochem Pharmacol 2023;208:115407.
31. Jiang J, Chen Q, Chen X, et al. Magnesium sulfate ameliorates sepsis-induced diaphragm dysfunction in rats via inhibiting HMGB1/TLR4/NF-κB pathway. Neuroreport 2020;31:902-8.
32. Zhang GY, Lu D, Duan SF, et al. Hydrogen Sulfide Alleviates Lipopolysaccharide-Induced Diaphragm Dysfunction in Rats by Reducing Apoptosis and Inflammation through ROS/MAPK and TLR4/NF-κB Signaling Pathways. Oxid Med Cell Longev 2018;2018:9647809.
33. Smith IJ, Godinez GL, Singh BK, et al. Inhibition of Janus kinase signaling during controlled mechanical ventilation prevents ventilation-induced diaphragm dysfunction. FASEB J 2014;28:2790-803.
34. Marini JC, Forlino A, Bächinger HP, et al. Osteogenesis imperfecta. Nat Rev Dis Primers 2017;3:17052.

35. Baglole CJ, Liang F, Traboulsi H, et al. Pulmonary and diaphragmatic pathology in collagen type I α1 mutant mice with osteogenesis imperfecta. Pediatr Res 2018;83:1165-71.
36. You W, Liu S, Ji J, et al. Growth arrest and DNA damage-inducible alpha regulates muscle repair and fat infiltration through ATP synthase F1 subunit alpha. J Cachexia Sarcopenia Muscle 2023;14:326-41.
37. Supinski GS, Wang L, Schroder EA, et al. MitoTEMPOL, a mitochondrial targeted antioxidant, prevents sepsis-induced diaphragm dysfunction. Am J Physiol Lung Cell Mol Physiol 2020;319:L228-38.
38. Yan Y, Li M, Lin J, et al. Adenosine monophosphate activated protein kinase contributes to skeletal muscle health through the control of mitochondrial function. Front Pharmacol 2022;13:947387.
39. Yin D, Lin D, Xie Y, et al. Neuregulin-1β Alleviates Sepsis-Induced Skeletal Muscle Atrophy by Inhibiting Autophagy via AKT/mTOR Signaling Pathway in Rats. Shock 2022;57:397-407.
40. Supinski GS, Alimov AP, Wang L, et al. Calcium-dependent phospholipase A2 modulates infection-induced diaphragm dysfunction. Am J Physiol Lung Cell Mol Physiol 2016;310:L975-84.

Cite this article as: Yuan X, Xue F, Yu Y, Cao X, Han Y, Wang F, Zhong L. The molecular mechanism of sepsis-induced diaphragm dysfunction. J Thorac Dis 2023;15(12):6831-6847. doi: 10.21037/jtd-23-1680